Fast Spectral Reflectance Recovery using DLP Projector

Shuai Han[1], Imari Sato[2], Takahiro Okabe[1], and Yoichi Sato[1]

[1] Institute of Industrial Science, The University of Tokyo, Japan
[2] National Institute of Informatics, Japan
{hanshuai,takahiro,ysato}@iis.u-tokyo.ac.jp, imarik@nii.ac.jp

Abstract. Spectral reflectance is an intrinsic characteristic of objects which is useful for solving a variety of computer vision problems. In this work, we present a novel system for spectral reflectance recovery with a high temporal resolution by exploiting the unique color-forming mechanism of DLP projectors. DLP projectors use color wheels to produce desired light. Since the color wheels consist of several color segments and rotate fast, a DLP projector can be used as a light source with spectrally distinct illuminations. And, the appearance of a scene under the projector's irradiation can be captured by a high-speed camera. Our system is built on easily available devices and capable of taking spectral measurements at 100Hz. Based on the measurements, spectral reflectance of the scene is recovered using a linear model approximation. We carefully evaluate the accuracy of our system and demonstrate its effectiveness by spectral relighting of dynamic scenes.

1 Introduction

The amount of light reflected on an object's surface varies for different wavelengths. The ratio of the spectral intensity of reflected light to incident light is known as the spectral reflectance. It is an intrinsic characteristic of objects that is independent of illuminations and imaging sensors. Therefore, spectral reflectance offers direct descriptions about objects that are useful to computer vision tasks, such as color constancy, object discrimination, relighting etc.

Several methods have been proposed for spectral reflectance recovery. Maloney used an RGB camera to recover the spectral reflectance under ambient illumination [1]. This method is limited by a low recovery accuracy due to its RGB 3-channel measurements. To get measurements that contain more than 3 channels, some works attach filters to a light source to modulate the illumination [2] or sequentially place a set of band-pass filters in front of a monochromatic camera to produce a multi-channel camera [3]. Since switching among filters is time-consuming, these methods are unsuitable for dynamic scenes. To increase temporal resolution, specially designed clusters of different types of LEDs were created [4]. The LED clusters work synchronously with an RGB camera for conducting spectral measurements at 30 fps. Since such self-made light sources, as

well as the controller for synchronization, are not easily available, a level of effort is required to build a similar system.

What we seek is a practical system for fast spectral reflectance recovery built on easily available devices. In this work, we exploit the unique color-forming mechanism of Digital Light Processing (DLP) projectors and apply it for spectral measurements. DLP projectors use color wheels to produce the desired light. The color wheels are composed of several color segments, and the light that gets through these segments has specific spectral distributions. In other words, DLP projectors provide several spectrally distinct illuminations. When the color wheels rotate quickly, the light emitted from the DLP projectors rapidly switches among these illuminations. Making use of this switch, we built an imaging system that takes spectral measurements with a high temporal resolution.

In the system, a DLP projector is used as a light source, and a high-speed camera is used to capture the scenes' appearance under the projector's irradiation. A standard diffuse white board is placed in the scene to recover the illumination spectra of the captured frames. In order to reduce the number of required measurements for an accurate spectral reflectance recovery, we represent the spectral reflectance as a linear combination of a limited number of spectral bases, which was done in previous studies [5, 6]. Using this linear model, the spectral reflectance of the scene points can be reconstructed by using every five consecutive captured frames.

The contributions of this work are summarized below.

- **Dense temporal spectral measurement:** Our system is capable of taking spectral measurements at 100 Hz. This enables measurement for the fast-moving objects, and the recovered results are degraded little by motion blur.
- **Easily built imaging system:** Considering that high-speed cameras are becoming readily available in end-user markets and no synchronization between the projector and the camera is required, our system can be easily replicated by others. Furthermore, using the DLP projectors as light sources, the irradiation uniformity within the entire projection plane can be guaranteed, so the calibrations are simple and the working volume is large.

This paper is organized as follows. Section 2 gives a brief review of the related works. Section 3 presents our imaging system and its use for spectral reflectance recovery. Section 4 verifies its accuracy. Section 5 shows the relighting results of a static scene and a moving object. We conclude this work in Section 6.

2 Related work

Spectral reflectance can be recovered under passive illumination. Maloney and Wandell used color constancy and an RGB camera for spectral reflectance recovery [1], but the accuracy of their method was low due to the RGB 3-channel measurement. For accurate results, Tominaga put a set of band-pass filters in front of a monochromatic camera, so that more than 3 channels can be measured [3]. However, this method trades off temporal resolution for the spectral resolution, and thus, is unsuitable for dynamic scenes.

Other existing methods for spectral reflectance recovery rely on active illumination. DiCalro and Wandell recovered the spectral reflectance as an intermediate result [7], but the accuracy was limited by the expression of the spectral reflectance as a combination of three spectral bases. To recover spectral reflectance with high accuracy, D'Zmura proposed a method using distinct illuminations[8], but the author only showed the results using synthetic data, and how well the proposed method works for real scenes was left unknown. Cui et al. proposed an algorithm for selecting an optimized set of wide-band filters and built a multi-illumination system [2]. They attached the selected filters to a light source, and used it as an additional light source for spectral reflectance recovery under ambient illumination. This method works well for static scenes. However, switching among different illuminations is time-consuming, so the system is not applicable for moving objects.

To measure the dynamic scenes, Park et al. built an imaging system based on multiplexed illumination [4]. They focused on the combinations of different LEDs and built LED clusters to capture 30 fps multi-spectral videos. However, their system requires specially built LED clusters and synchronization between the LED clusters and a camera. Accordingly, their system is not easily available. Moreover, using these self-made LED clusters, irradiation uniformity can be guaranteed only in a small area, so the working volume is quite limited.

Our work is also related to DLP-based active vision. Nayar et al. implemented a programmable imaging system using a modified DLP projector-camera pair [9]. Users can control the radiometric and geometric characteristics of the captured images by using this system. Narasimhan et al. exploited the temporal dithering of DLP projectors for a wide range of applications [10]. Zhang and Huang used the fast illumination variation of a DLP projector for real-time 3D shape measurements [11]. These three works only utilized the fast alternation between the "on" and "off" statuses of the digital micromirror device in a DLP projector; the spectral information was disregarded. In contrast, we use the spectral information from the emitted light for the spectral reflectance recovery. Our work is the first to recover spectral reflectance using a DLP projector.

3 Spectral Reflectance Recovery

3.1 Three steps for spectral reflectance recovery

There are three factors related to image brightness: the incident light, the scene, and the camera. Suppose the camera has a linear intensity response, this relationship can be expressed as

$$I_{m,n} = \int s(\lambda) c_m(\lambda) l_n(\lambda) d\lambda, \tag{1}$$

where λ is the wavelength, $I_{m,n}$ is the intensity of a scene point in a captured frame, $s(\lambda)$ is the spectral reflectance of that point, $c_m(\lambda)$ is the spectral response function of the camera at the mth color channel, and $l_n(\lambda)$ is the spectrum of the nth illumination.

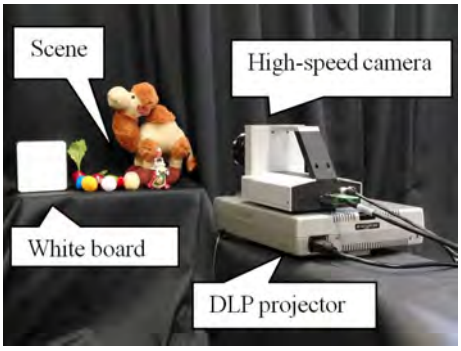

Fig. 1. Prototype System. Composed of a DLP projector (PLUS^{TM}U2-1130), a high-speed camera (PointGrey^{TM} Lightning) and a white board (labsphere^{TM} SRT-99).

The goal of this work is to recover spectral reflectance $s(\lambda)$ in a visible range $(400--700[\text{nm}])$. From Eq. 1, we can see that a large set of spectrally distinct measurements are required if we want to recover $s(\lambda)$ with high spectral resolution. To reduce the number of required measurements without sacrificing spectral resolution, we approximate the spectral reflectance as a combination of a limited number spectral basis functions. This approximation procedure was also used in former works [4, 7].

Several linear models [5, 6] and a nonlinear model [12] have been built by using principal component analysis [13] or other tools (see Ref. [14] for a review about surface reflectance approximation). With regard to how many bases are required for accurate reconstruction, different works have different conclusions [5, 6, 15–17]. We adopt an 8-dimension linear model for spectral reflectance derived from Ref. [6] on account of its high reconstruction accuracy. On the basis of this linear model, the spectral reflectance is represented as

$$s(\lambda) = \sum_{j=1}^{8} \alpha_j b_j(\lambda), \tag{2}$$

where $b_j(\lambda)(j = 1, 2, .., 8)$ is the jth spectral basis from Ref. [6] (spectral resolution:10nm), α_j is the corresponding coefficient. Substituting Eq.2 for Eq.1, we obtain

$$I_{m,n} = \sum_{j=1}^{8} \alpha_j \int b_j(\lambda) c_m(\lambda) l_n(\lambda) d\lambda \tag{3}$$

In this work, we first estimate α_j from observed $I_{m,n}$. Then, spectral reflectance $s(\lambda)$ is reconstructed by substituting α_j into Eq. 2.

As shown in Fig. 1, our imaging system is composed of a one-chip DLP projector, a high-speed RGB camera with a linear intensity response and a standard

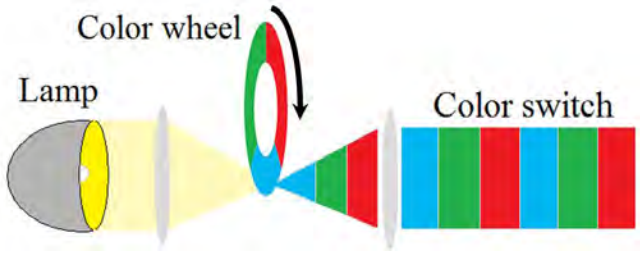

Fig. 2. Color switch caused by rotation of color wheel.

diffuse white board. Using this system, we do spectral reflectance recovery in the follow three steps.

1. Image acquisition: Scene's appearance under the projector's irradiation $I_{m,n}$, is acquired by using the high-speed camera. Every five consecutive frames are used as one measurement for the spectral reflectance recovery. (Section 3.2)

2. Illumination recovery: Illumination spectra $l_n(\lambda)$, changes from frame to frame. We use the diffuse white board as a calibration target to recover the illumination of captured frames. (Section 3.3)

3. Spectral reflectance reconstruction: Based on the 8-dimensional linear model, spectral reflectance $s(\lambda)$, can be reconstructed from the acquired images and recovered illuminations. (Section 3.4)

We explain each of these steps in detail in the following parts.

3.2 Image acquisition by color switch

Different from other kinds of projectors, DLP projectors use color wheels to produce the desired light. The color wheel consists of several color segments, and these segments only allow light in a specific wavelength range to get through. When the color wheel quickly rotates, the light emitted from DLP projectors changes rapidly. In our work, this temporal variation in light is referred to as "color switch". A diagrammatic sketch is shown in Fig. 2. In our system, a DLP projector equipped with a 3-segment color wheel has been used (PLUS$^{\mathrm{TM}}$U2-1130). since the color wheel rotates at 120 rps (round per second), color switch occurs at 360 Hz (3×120).

The human eyes, and common video cameras work at low rates ($24--30$ [Hz]), and thus they cannot detect the color switch. In this work, a 500 fps camera (PointGrey$^{\mathrm{TM}}$ Lightning) is adopted to take images of scenes under the projector's irradiation. The camera outputs 24bit (8×3) color images at a SXGA resolution (1280×1024), and its linear intensity response can be verified by adjusting the shutter speed. In addition, the spectral response function of the camera $c_m(\lambda)$ ($m = 1, 2, 3$), was measured by using a monochromator and a spectrometer. The monochromator is used to generate a sequence of narrow-band lights. The spectral radiance of these lights is measured by the spectrometer. We

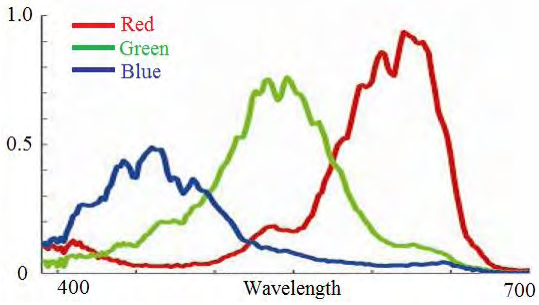

Fig. 3. Camera's spectral response function for RGB 3 channels.

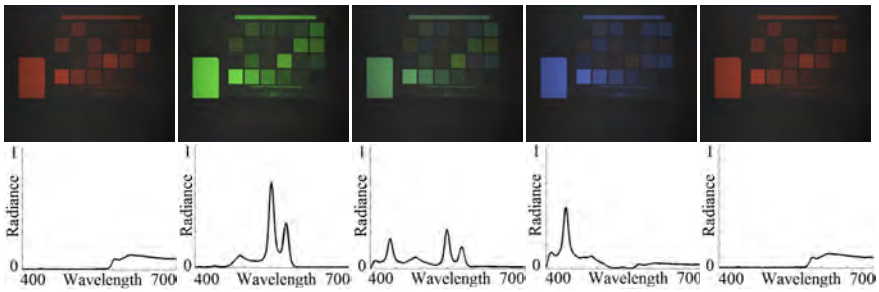

Fig. 4. One measurement of Macbeth ColorChecker and corresponding illumination spectra. Top row: 5 frames captured sequentially by the 500 fps camera in 1/100s. Bottom row: recovered illuminations of corresponding frames.

expose the camera's sensor to the narrow-band lights and capture images. The relationship between the RGB values in the captured images and the spectral radiance of the corresponding lights, i.e., spectral response function, is shown in Fig. 3. During one rotation of the color wheel, the high-speed camera can capture 4.17 frames. So, we use five consecutive frames as one measurement for the spectral reflectance recovery. Fig. 4 shows one measurement about Macbeth ColorChecker. We can see that the scene's appearance clearly changes under the color switch of the DLP projector. It should be noted that the color switch occurs at 360Hz, but the camera operates at 500 fps, so the projector and the camera work asynchronously.

3.3 Illumination recovery

Our system does not require synchronization between the projector and the camera. Due to the asynchronism, the illumination changes from frame to frame. In this section, we describe how to recover the illumination spectrum $l_n(\lambda)$ of

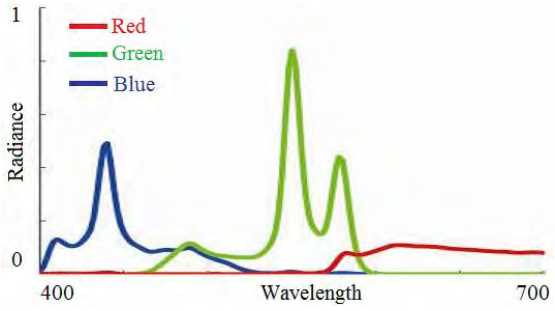

Fig. 5. Spectra of three distinct illuminations of the DLP projector.

every frame using a standard diffuse white board (labsphere^{TM} SRT-99) placed within the scene as a calibration target.

As mentioned above, light that gets through different segments on color wheels has distinct spectral distributions. If we use these spectral distributions as the illumination bases, light emitted from the DLP projectors can be expressed by a linear combination of these bases. In our system, since the three segments of the color wheel correspond to the RGB color filters, we can acquire these three distinct illuminations by inputting the projector (255, 0, 0), (0, 255, 0), and (0, 0, 255) respectively. Their spectra, which are measured by a spectrometer, are shown in Fig. 5. For each frame, its illumination spectrum ,$l_n(\lambda)$, can be represented as

$$l_n(\lambda) = \sum_{k=1}^{3} \beta_{n,k} p_k(\lambda), \text{ subject to } \beta_{n,k} > 0, \tag{4}$$

where $p_k(\lambda)$ is the spectrum of the kth illumination basis of the DLP projector, $\beta_{n,k}$ is the corresponding coefficient.

By using Eqs.1 and 4, the brightness of a surface point on the white board is

$$I^w_{m,n} = \sum_{k=1}^{3} \beta_{n,k} \int p_k(\lambda) s^w(\lambda) c_m(\lambda) d\lambda, \tag{5}$$

where $I^w_{m,n}$ is the intensity of that point, and $s^w(\lambda)$ means its spectral reflectance. Use $P_{k,m}$ to represent the intensity of the point at the mth channel under the kth illumination basis

$$P_{k,m} = \int p_k(\lambda) s^w(\lambda) c_m(\lambda) d\lambda \ (k = 1, 2, 3), \tag{6}$$

Eq. 5 can be rewritten as

$$I^w_{m,n} = \sum_{k=1}^{3} \beta_{n,k} P_{k,m}, \tag{7}$$

$P_{k,m}(k = 1, 2, 3)$ can be measured by using the high-speed camera to capture images of the white board under three distinct illuminations of the projector. We only need to measure them once in advance.

From Eq. 7, we see that the intensity of a surface point on the white board under illumination $l_n(\lambda)$ is a linear combination of its intensities under three illumination bases

$$\boldsymbol{I}_n^w = \left[I_{1,n}^w \; I_{2,n}^w \; I_{3,n}^w\right]^T = \boldsymbol{P}^w \boldsymbol{\beta}_n, \tag{8}$$

where $\boldsymbol{I}_n^w$ represents the RGB value of a surface point on the white board under the nth illumination, $\boldsymbol{P}^w$ is a 3×3 matrix consists of $P_{k,m}(k = 1, 2, 3,\ m = 1, 2, 3)$, $\boldsymbol{\beta}_n$ is the corresponding 3×1 coefficient vector.

In principle, $\boldsymbol{\beta}_n$ can be easily calculated by $\boldsymbol{\beta}_n = (\boldsymbol{P}^w)^{-1}\boldsymbol{I}_n^w$. However, due to the noise , $\beta_{n,k}$ $(k = 1, 2, 3)$ may sometimes be negative. This conflicts with the non-negative constraint of Eq. 4. Thus, we solve $\boldsymbol{\beta_n}$ as a non-negative least squares problem:

$$\boldsymbol{\beta}_n = \underset{\boldsymbol{\beta}_n}{argmin} \mid \boldsymbol{I}_n^w - \boldsymbol{P}^w \boldsymbol{\beta}_n \mid^2, \quad \text{subject to } \beta_{n,k} \geq 0 \; (k = 1, 2, 3) \tag{9}$$

Using calculated $\boldsymbol{\beta_n}$, illumination spectrum $l_n(\lambda)$ can be reconstructed by using Eq.4.

3.4 Spectral reflectance reconstruction using constrained model

Since $l_n(\lambda)$ is recovered in Section 3.3, the integral in Eq. 3 can be represented as known coefficients: $f_{j,m,n} = \int b_j(\lambda) c_m(\lambda) l_n(\lambda) d\lambda$. One measurement that contains five consecutive frames can be written in matrix form as

$$\boldsymbol{I} = \boldsymbol{F}\boldsymbol{\alpha}, \tag{10}$$

where $\boldsymbol{I}$ is a 15×1 vector (15 measurements: RGB 3 channels $\times$ 5 frames), $\boldsymbol{F}$ is a 15×8 matrix (15 measurements $\times$ 8 spectral bases), and $\boldsymbol{\alpha}$ is an 8×1 coefficient vector.

If $\boldsymbol{\alpha}$ is estimated from $\boldsymbol{I}$, spectral reflectance $s(\lambda)$ can be reconstructed by Eq. 2. In this way, the problem of spectral reflectance recovery can be solved by the 8 coefficients estimation. The DLP projector in our system has three spectrally distinct illuminations, and the high-speed camera provides a 3-channel measurement under each illumination. In total, we can obtain 3×3, i.e., 9 effective channels. Thus, the problem of estimating 8 coefficients is over-determined. However, using the least squares solution in Eq. 10, the reconstructed spectral reflectance does not always satisfy the non-negative constraint and the solutions tend to be unstable. Therefore, we adopted the constrained minimization method proposed in Ref. [4]. We use the first derivative of the spectral reflectance respective to λ as the constraint:

$$\boldsymbol{\alpha} = \underset{\boldsymbol{\alpha}}{argmin} \left[\mid \boldsymbol{I} - \boldsymbol{F}\boldsymbol{\alpha} \mid^2 + \gamma \mid \frac{\partial s(\lambda)}{\partial \lambda} \mid^2 \right], \text{subject to } \boldsymbol{b_m}\boldsymbol{\alpha} \geq 0 \text{ for all } \lambda, \tag{11}$$

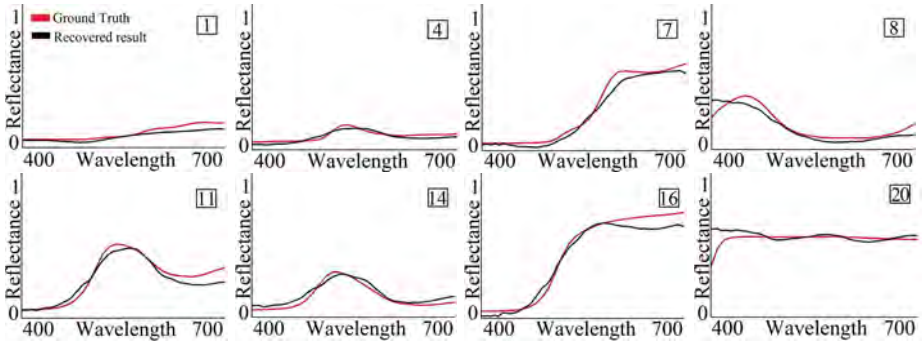

Fig. 6. Recovered spectral reflectance of some clips on Macbeth ColorChecker by the measurement shown in Fig. 4. Ground truth: red lines; recovered: black lines.

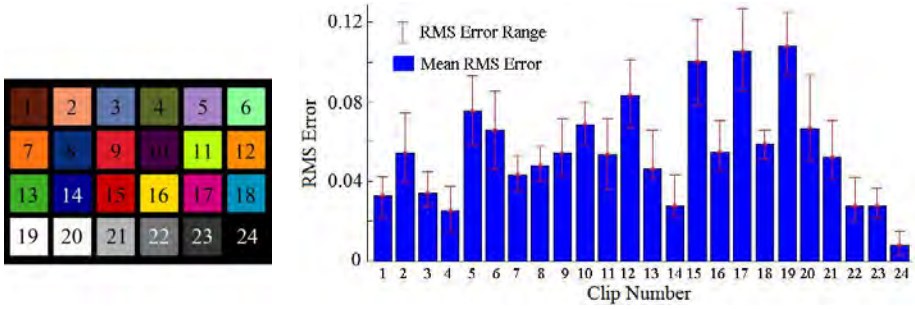

Fig. 7. RMS error of 24 clips of Macbeth ColorChecker for 200 measurements.

where γ is a weight for the constraint term. $\boldsymbol{b_m}$ is a 31×8 matrix whose columns are the 8 spectral bases.

4 Accuracy Evaluation

In this section, we evaluate the accuracy of our system by using Macbeth ColorChecker. In the system, every five consecutive frames captured by the 500 fps camera are used as one measurement. Thus, the spectral measurements are taken at 100 Hz. But, the color wheel rotates at 120 rps. Due to the asynchronism between the DLP projector and the camera, frames captured at different times have different illumination spectra. The accuracy of the recovered results would be affected by this temporal illumination variation. Thus, we need to evaluate both the spectral accuracy and temporal accuracy of our system in this section.

We sequentially took 200 measurements (1000 frames) of a static 24-clip Macbeth ColorChecker to evaluate spectral accuracy. For each clip, we set γ in Eq. 11 to 50 and reconstructed its spectrum based on the measurements (some results are shown in Fig. 6); then, the root mean square (RMS) error of all 200

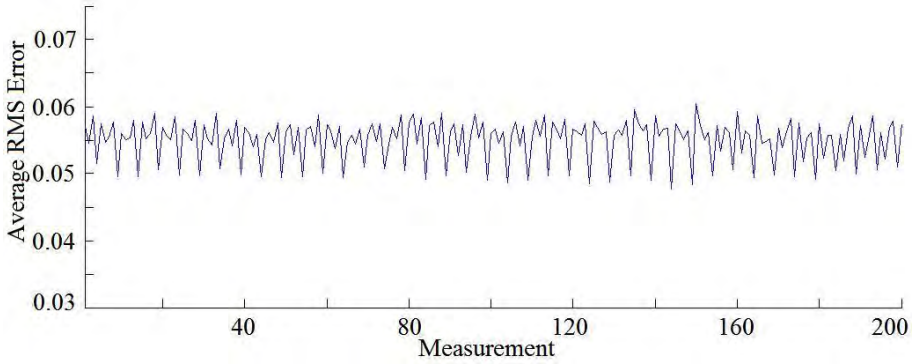

Fig. 8. Average RMS error for 200 measurements. Because color wheel rotates 6 rounds for every 5 measurements, a pattern of the average RMS error can be seen.

reconstructed results was calculated. We also computed the maximum, mean, and minimum among the 200 RMS error values for every clip. The results for all 24 clips are shown in Fig. 7. We can see that, for all clips, their maximum RMS error does not deviate a lot from the minimum one. In addition, the biggest mean RMS error of all 24 clips is less than 0.11. These results demonstrate that our system can recover the spectral reflectance at a reasonable accuracy.

Next, we evaluated the temporal accuracy of our system. We reused the 200 measurements taken in previous test. For every measurement, we reconstructed the spectral reflectance of all 24 clips; then, the RMS error of the 24 reconstructed results was calculated; after that, we computed the average value of the 24 RMS error values, and used it as the criterion to evaluate each measurement. The results for all 200 measurements are shown in Fig. 8. The average value fluctuates in a narrow band (0.047, 0.06) which verifies the temporal accuracy of our system.

5 Image and Video Relighting

We used the spectral reflectance recovered by our method to do spectral relighting of a static scene as well as a moving object. To ensure there was a strong and spatial uniformly distributed light, an LCD projector (EPSON^{TM} ELP-735) was used as the light source for relighting. The spectral distributions of its white, red, green, and blue were measured by a spectrometer.

5.1 Image relighting

We set a static scene with fruits, vegetables, and small statues. Five consecutive frames from the scene were captured by our imaging system. Using them as one measurement, the spectral reflectance of scene points was recovered pixel by pixel. Then, the scene was spectrally relit by using Eq. 1 with the known

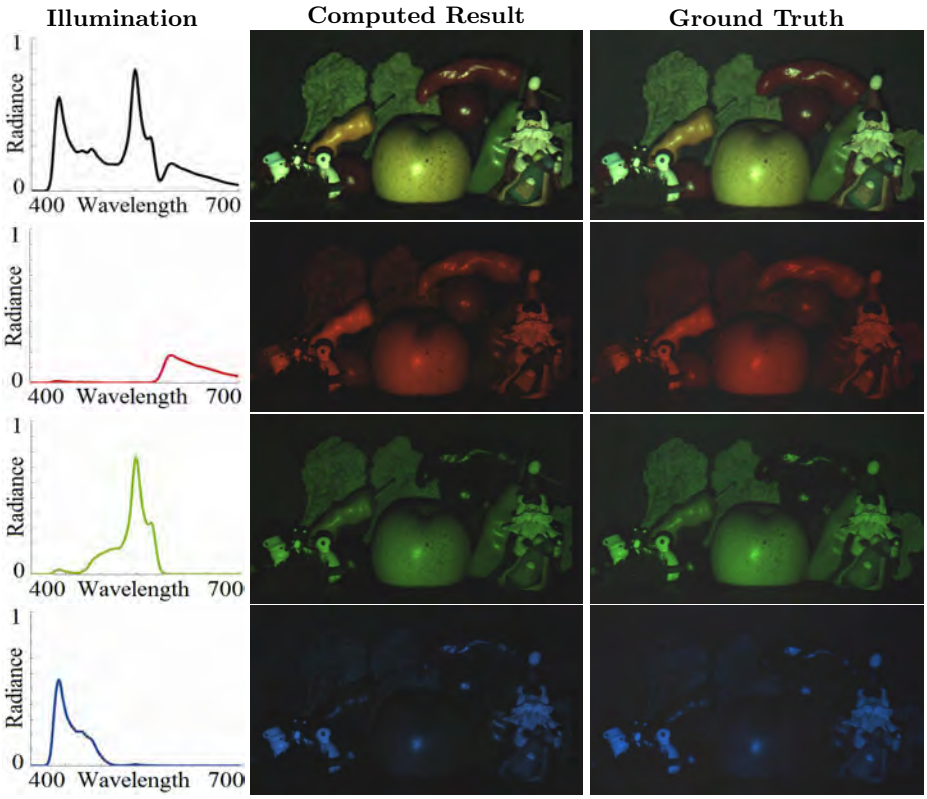

Fig. 9. Comparison between relit results and captured images of static scene under illuminations from a LCD projector.

illumination spectra of the LCD projector. A comparison between the relit results and the real captured images is shown in Fig. 9. We can see from the comparison that the computed results are very similar to the ground truth, which also reveals the accuracy of our system.

5.2 Real video relighting

Our system works at 100 Hz, so it is capable of measuring dynamic scenes. This capability was tested by taking spectral measurements of a manipulated toy consequently. For every measurement, the spectral reflectance of scene points was reconstructed. Based on the recovered data, the toy's movements were spectrally relit under a variety of illuminations. The results are shown in the top two rows of Fig. 10, and we can that there is a smooth movement, and the computed results look natural. In the bottom of Fig. 10, a relit result is shown in the middle. It was computed on the basis of the spectral data recovered by our system. The left is a image captured by the high-speed camera under the LCD projector's

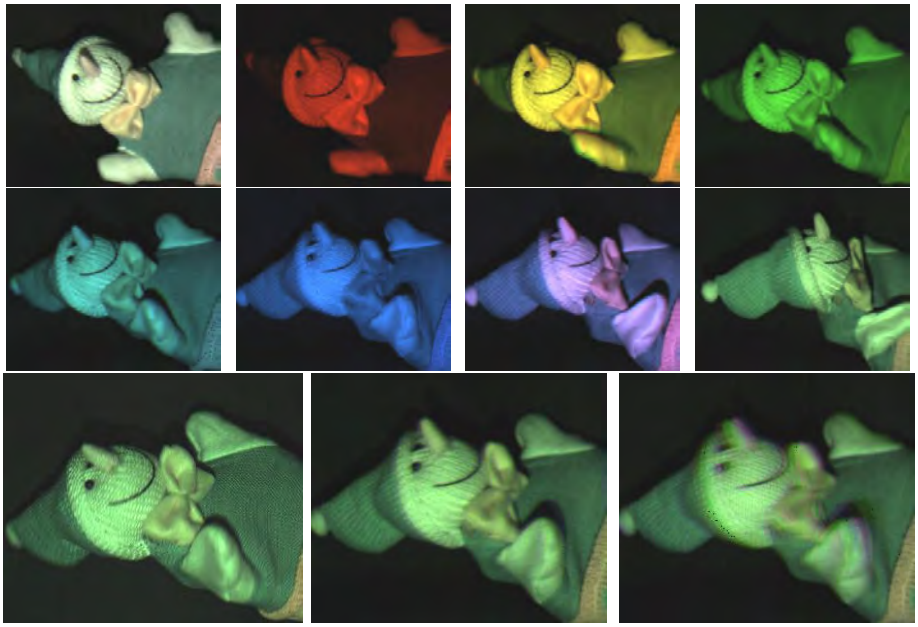

Fig. 10. Top two rows: relit results of fast-moving toy. The continuous movements through very different illuminations are shown. Bottom row: on the left is an image captured by the 500 fps camera, the middle is relit result, and the right is synthesized result to simulate captured image by a 30 fps camera. The recovered result by our system is only slightly degraded by motion blur.

irradiation. A synthesized result to simulate captured image by a 30 fps camera is shown on the right side. Through comparisons, we can see that the relit result resembles the real captured image, and it is degraded little by the motion blur which is obvious in the synthesized result. From the comparisons, we can see that our system is robust to artifacts caused by motion. Therefore, our system is suitable for spectral reflectance recovery of dynamic scenes.

6 Conclusion

In this work, we exploited the unique color-forming mechanism of DLP projectors. An imaging system for fast spectral reflectance recovery was built by making use of this mechanism. This system is capable of taking measurements as fast as 100 Hz. Every measurement consists of a set of sequentially captured images. For each set, the spectral reflectance of scene points can be recovered. Through intensive evaluation, the accuracy and the robustness of our system have been verified. Moreover, our system is built on easily available devices, and the excellent optical design of DLP projectors guarantees simple calibrations and

a large working volume. It can be concluded that our system is practical and robust for the spectral reflectance recovery of fast-moving objects.

Acknowledgement

This research was supported in part by Grant-in-Aide for Scientific Research on Innovative Areas from the Ministry of Education, Culture, Sports, Science and Technology.

References

1. L. T. Maloney and B. A. Wandell: Color constancy: a method for recovering surface spectral reflectance. Journal of the Optical Society of America A 3 (1986) 29-33
2. C. Chi, H. Yoo and M. Ben-Ezra: Multi-spectral imaging by optimized wide band illumination. International Journal on Computer Vision 86 (2010) 140-151
3. S. Tominaga: Multichannel vision system for estimating surface and illumination functions. Journal of the Optical Society of America A 13 (1996) 2163-2173
4. J. Park, M. Lee and M. D. Grossberg and S. K. Nayar: Multispectral Imaging Using Multiplexed Illumination. In: Proc. IEEE International Conference on Computer Vision (2007)
5. J. Cohen: Dependency of the spectral reflectance curves of the munsell color chips. Psychon. Science 1 (1964) 369-370
6. J. P. S. Parkkinen, J. Hallikainen and T. Jaaskelainen: Characteristic spectra of munsell colors. Journal of the Optical Society of America A 6 (1989) 318-322
7. J. M. DiCarlo and B. A. Wandell: Illuminating illumination. In: Proc. Ninth Color Imaging Conference (2000) 27-34
8. M. D'Zmura: Color constancy: surface color from changing illumination. Journal of the Optical Society of America A 9 (1992) 490-493
9. S. K. Nayar, V. Branzoi and T. E. Boult: Programmable imaging: Towards a flexible camera. International Journal on Computer Vision 70 (2006) 7-22
10. S. G. Narasimhan, S. J. Koppal and S. Yamazaki: Temporal dithering of illumination for fast active vision. In: Proc. European Conference Computer Vision (2008)
11. S. Zhang and P. Huang: High-resolution, real-time 3d shape acquisition. In: Proc. IEEE Conference on Computer Vision and Pattern Recognition Workshops. Volume 3 (2004) 28-37
12. J. M. DiCarlo and B. A. Wandell: Spectral estimation theory: beyond linear but before Bayesian. Journal of the Optical Society of America A 20 (2003) 1261-1270
13. D. Tzeng and R. S. Berns: A review of principal component analysis and its applications to color technology. Color Research And Application 30 (2006) 84-98
14. O. Kohonen, J. Parkkinen and T. Jääskeläinen: Databases for spectral color science. Color Research And Application 31 (2006) 381-390
15. J. L. Dannemiller: Spectral reflectance of natural objects: how many basis functions are necessary? Journal of the Optical Society of America A 9 (1992) 507-515
16. C. Chiao, T. W. Cronin and D. Osorio: Color signals in natural scenes: characteristics of reflectance spectra and effects of natural illuminants. Journal of the Optical Society of America A 17 (2000) 218-224
17. L. T. Maloney: Evaluation of linear models of surface spectral reflectance with small numbers of parameters. Journal of the Optical Society of America A 3 (1986) 1673-1683